Immobilizing Laccase on Kaolinite and Its Application in Treatment of Malachite Green Effluent with the Coexistence of Cd (II)

Xiaofeng Wen [a,1], Chunyan Du [b,c,1], Jia Wan [a,1], GuangmingZeng [a*], Danlian Huang [a*], Lingshi Yin [b,c], Rui Deng [a], ShiyangTan [b,c], Jinfan Zhang [b,c]

[a] College of Environmental Science and Engineering, Hunan University and Key Laboratory of Environmental Biology and Pollution Control (Hunan University), Ministry of Education, Changsha 410082, P.R. China;

[b] School of Hydraulic Engineering, Changsha University of Science &Technology, Changsha 410114, P.R. China;

[c] Key Laboratory of Water-Sediment Sciences and Water Disaster Prevention of Hunan Province, Changsha 410114, P.R. China;

*Corresponding author.

E-mail address: zgming@hnu.edu.cn (G.M.Zeng), huangdanlian@hnu.edu.cn (D.L. Huang). *Tel.*: +86 731 88823701. *Fax:* +86 731 88823701.

1 These authors contribute equally to this article.

ABSTRACT： Malachite green effluent with the Coexistence of Cd (Π) was efficiently decolorized by kaolinite-*laccase* (Kaolin-*Lac*). Laccase from *Trametes versicolor* was immobilized onto the kaolinite through physical adsorption contact. The optimal conditions were 180 min of immobilization time and 0.8 mg/mL of enzyme solution. Kaolin-*Lac* could obtain a loading efficiency of 88.22%, a loading capacity of 12.25 mg/g, and the highest activity of 839.01 U/g. Moreover, the process of immobilization increased its pH stability and operational stability. Kaolin-*Lac* retained above 50% of the original activity and nearly 80% decolorization for MG after 5 cycles. In the presence of 3, 5-Dimethoxy-4-hydroxybenzaldehyde (SA), Kaolin-*Lac* could degrade over 98% of malachite green. The coexistence of Cd (Π) was beneficial to the decolorization of malachite green by Kaolin-*Lac*. The structural and morphological features of kaolinite, Kaolin-*Lac* and Kaolin-*Lac* after degradation were determined by scanning electron microscopy-energy spectrum analysis (SEM-EDS) and Fourier transform infrared spectroscopy (FTIR). Cadmium appeared on the Kaolin-*Lac* after degradation. After immobilization and degradation, the surface groups on kaolinite were changed. Kaolin-*Lac* showed its more potential continuous employment than free laccase in practical malachite green dyes effluent mixed with Cd (Π).

KEYWORDS： *Malachite Green, Cd (II), Coexistence, Laccase immobilization, Kaolinite, Removal*

1. Introduction

Immobilization could improve laccase properties and it is an effective way to overcome the application limitations of laccase, such as low stability and high production costs (Mohamad et al., 2015; Prasad and Palanivelu, 2015). The exploration of immobilization methods of laccase has been predominantly focused (Barbosa et al., 2013; Guzik et al., 2014). The immobilization methods can increase the stability of laccases, thus significantly reducing the cost burden (Datta et al., 2013; Sheldon and van Pelt, 2013).

In the laccase immobilization process, various carriers have been reported to immobilize laccase successfully (An et al., 2015; Tan et al., 2015). Among various carriers, kaolinite as an alumino-silicate mineral is cost-efficient, facility of reusability, low mass transfer resistance and microbial corrosion resistance (Abdul Rahman et al., 2005; Hu et al., 2007). Kaolinite has negative sites on the basal surface owing to isomorphic substitution and amphoteric sites on the edge surface (Liang et al., 2017; Shu et al., 2016). The amphoteric sites are conditionally charged and pH dependent because a net positive or net negative charge can be produced due to proton adsorption (An et al., 2015; Zhang et al., 2015). Kaolinite has a low permanent charge and a

significant variable charge (Sinegani et al., 2005; Xu et al., 2012). Attributing to these distinctive characters, kaolinite has rather high adsorption ability. Kaolinite is widely used in adsorption studies.

Malachite green (MG) was produced from the textile staining, aquaculture, food and medical domains (Chen et al., 2015; Sinha and Osborne, 2016). The MG belongs to persistent contaminant, and it can be readily adsorbed on solid or absorbed by organism thus leading to the accumulations in organisms (Gong et al., 2009). The accumulation of MG hinders organisms' growth, reproduction and development, and they can generate mutagenic and carcinogenic influence. Furthermore, the MG effluent is always released to environment combining with heavy metals like Cd (Π) in realistic situations (Deng et al., 2013; Jasinska et al., 2012). The Cd (Π) has been listed as one of the top toxic heavy metals since it can cause cancer, bone lesions, lung insufficiency, anemia, hypertension and weight loss (Long et al., 2011; Wan et al., 2018). Elevated level of Cd (Π) could lead to the acute and chronic disorders in nervous, kidney, liver and cardiovascular system, therefore, efficient removal of Cd (Π) makes sense (Tang et al., 2014; Wu et al., 2017). The mixing of Cd (Π) makes the MG effluent more difficult to treat (Ren et al., 2018; Xu et al., 2012).

The redox-mediated bio-oxidation of MG, catalyzed by immobilized laccase, is a current technology for MG degradation (Kuhar et al., 2015; Zhang et al., 2016). Utilizing laccase immobilized on numerous carriers to catalyze MG degradation is an effective and straight forward method (Zhou et al., 2018). There are varieties of carriers, including chitosan beads, PAN/O-MMT composite nanofibers, a sponge-like hydrogel, and amino-functionalized magnetic nanoparticles were applied to immobilize laccase to degrade the MG effluent (Kumar et al., 2014; Li et al., 2016; Sun et al., 2015; Zheng et al., 2016). However, immobilizing laccase from *Trametes versicolor* on kaolinite to degrade MG effluent with the coexistence of Cd (II) was not fully explored. The existence of Cd (II) does have effect on the activity of free laccase and the degradation of MG by laccase (Cheng et al., 2016). Furthermore, during the laccase immobilization process, immobilization carrier also has important effect on laccase activity and stability (Zheng et al., 2016). Hence, whether if utilizing kaolinite to immobilize laccase from *Trametes versicolor* could degrade MG effectively, if the coexistence of Cd (II) could affect the degradation of MG and what is the remove efficiency of Cd (II) by immobilized laccase on kaolinite should be fully explored.

In the current study, kaolinite that has rather high adsorption ability was used for

laccase physical adsorption immobilization. The efficiency of loaded laccase on kaolinite was characterized by relative activity (%) and stability studies. Kaolinite-*laccase* (Kaolin-*Lac*) was applied in continuous treatment of MG effluent mixed with Cd (Π) in the presence of redox mediators SA to explore the removal efficiency of MG and Cd (II) by Kaolin- *Lac*, the effect of Cd (II) on the degradation efficiency of MG by Kaolin- *Lac*. The detailed characterizations changes of kaolinite, Kaolin-*Lac*, Kaolin-*Lac* after treatment were carried out by FT-IR, SEM-EDS.

2. Materials and methods

2.1. Materials

Laccase from *Trametes versicolor*, 3, 5-Dimethoxy-4-hydroxybenzaldehyde(SA) and 2,2-azino-bis(3-ethylbenzothiazoline-6-sulfonic acid) (ABTS) were obtained from Sigma-Aldrich. Malachite Green (MG) and Kaolinite were provided by Sinopharm Chemical Reagent Shanghai (China). All other chemicals were of analytical grade and were used as received without further purification.

2.2. Enzyme activity assay

Laccase activity was tested by analyzing the product formation rate of ABTS at the absorbance of 420 nm. One unit of laccase activity was defined as the amount of free

laccase required to oxidize 1 μM of substrate per minute. The activity of laccase in this study was expressed as the relative activity (%). During the immobilization and stability assessing process, the maximal value of laccase activity under each certain condition (such as a certain laccase concentration, immobilizing time or pH) was set as 100 % (Liu et al., 2012; Zheng et al., 2016).

2.3. Immobilization of Laccase

The immobilization process was carried out by the physical adsorption contact (such as ion exchange adsorption, hydrogen bond adsorption, and Vander waals adsorption) of kaolinite and laccase. Kaolinite was added in 5 mL of citrate phosphate buffer (0.1 M, pH 5) containing laccase (0.01, 0.05, 0.5, 0.8, 1 mg/mL). The mixtures were incubated in a rotary shaker at 30 ℃ and shake at 200 rpm for 15, 30, 60, 120, 180, 300 min. Then, the sample was centrifuged and the bottom solid was collected to wash a few times with buffer. The final solid was kaolin-*Lac* after freeze drying at -100 ℃ for 12 h. The Fig. 1 demonstrated the process of immobilization.

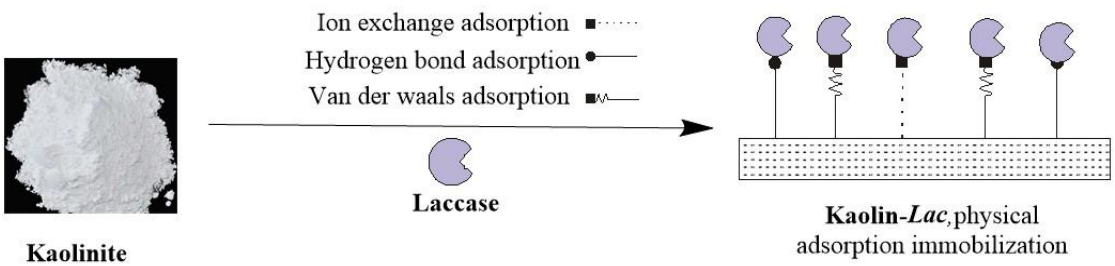

Fig.1 The process of laccase immobilized on kaolinite.

2.4. Stability Assessment.

2.4.1. pH stability of immobilized laccase

The pH value has great influence on the laccase activity. For pH stability, the samples were added to tubes that contained buffers (pH range of 3 to 6) and incubated at 30 ℃ and kept at 200 rpm. The residual enzyme activity of samples was determined.

2.4.2. Thermal stability of immobilized laccase

The thermal stability of immobilized laccase and free laccase were assessed. Free and immobilized laccase were kept from 30 ℃ to 80 ℃. Then the free and immobilized laccase were separately reacted with ABTS and centrifuged and the absorbance of supernatant was measured at 420 nm.

2.4.3. Storage stability of immobilized laccase

To test the storage stability, the immobilized laccase and free laccase samples were stored at 4 ℃ for 30 days of incubation cycles and residual activities were measured at every 5 day.

2.4.4. Operational stability of immobilized laccase

Kaolin-*Lac* was dispersed incitrate-phosphate buffer (pH 5) containing 1 mM

ABTS and cultured for 5 min. The sample was centrifuged and the content of transformed ABTS in the supernatant was determined. The Kaolin-*Lac* was washed with citrate-phosphate buffer, decanted and the procedure was repeated for 5 cycles.

2.5. Immobilized Laccase System for Treatment of MG Effluent mixed with Cd (II)

The decolorization efficiency of MG by Kaolin-*Lac* was analyzed by the decrease in absorbance at the absorption wavelength of 623 nm. The removal capacity of Cd (II) was analyzed by atomic absorption spectrophotometer (AAS). Effect of parameters such as the concentration of SA and Cd (II), reaction time were studied. The reaction mixture, containing kaolin-*Lac* and 10 mg/L of MG and Cd (II) solution, was incubated at 30 ℃. After centrifuged, the residual contaminants concentration in the supernatant was analyzed. All the experiments were examined in triplicate.

2.6. Characterization Analytical Methods

The SEM imaging was applied to characterize kaolinite, kaolin-*Lac* before and after degradation. The sample was gold-coated using a sputter coater before imaging. Micrographs were captured at 20 kV accelerating voltage on a scanning electron micro scope (FEI, QUANTA F250). Elemental analysis was determined with electronic differential system (EDAX, GENESIS). FT-IR spectra were recorded in the range of

500–4000 cm^{-1} by a Nicole 5700 FT-IR Spectrometer.

3. Results and discussion

3.1. Characterization analysis

3.1.1. SEM and elements analysis

The SEM aimed to observe possible morphological changes of kaolinite, Kaolin-*Lac*, and Kaolin-*Lac* after degradation. Kaolinite, it is a 1:1 type swelling clay (Huang et al., 2017a; Shu et al., 2016). The kaolinite lattice layers are made up of tetrahedral Si-O and octahedral Al-O. They are connected with the van der waals' forces. The structure lamella is filled with commutative cations and water molecules (Huang et al., 2018a; Shu et al., 2014).They can be replaced by ion exchange and inter layer exchange (Shu et al., 2016).The morphology of kaolinite and Kaolin-*Lac* samples has been displayed on the SEM images (Fig.2). There was no obvious distinction of different surface morphologies can be observed directly. The relevant EDS confirmed no obvious elements changed after immobilization in Fig.2a and Fig.2b. However, the relevant EDS in Fig.2c revealed elemental difference of Kaolin-*Lac* after treatment of MG effluent with Cd (Π). The appearance of cadmium (Cd) in Fig. 2c relevant EDS visually indicated the Cd (Π) was adhered to Kaolin-*Lac* external and internal pore

through adsorption. For the sake of preferably comprehending the formation element of materials, the percentages of seven mainly changed elements which are carbon, oxygen, sodium, magnesium, aluminum and calcium are listed in Table 1.

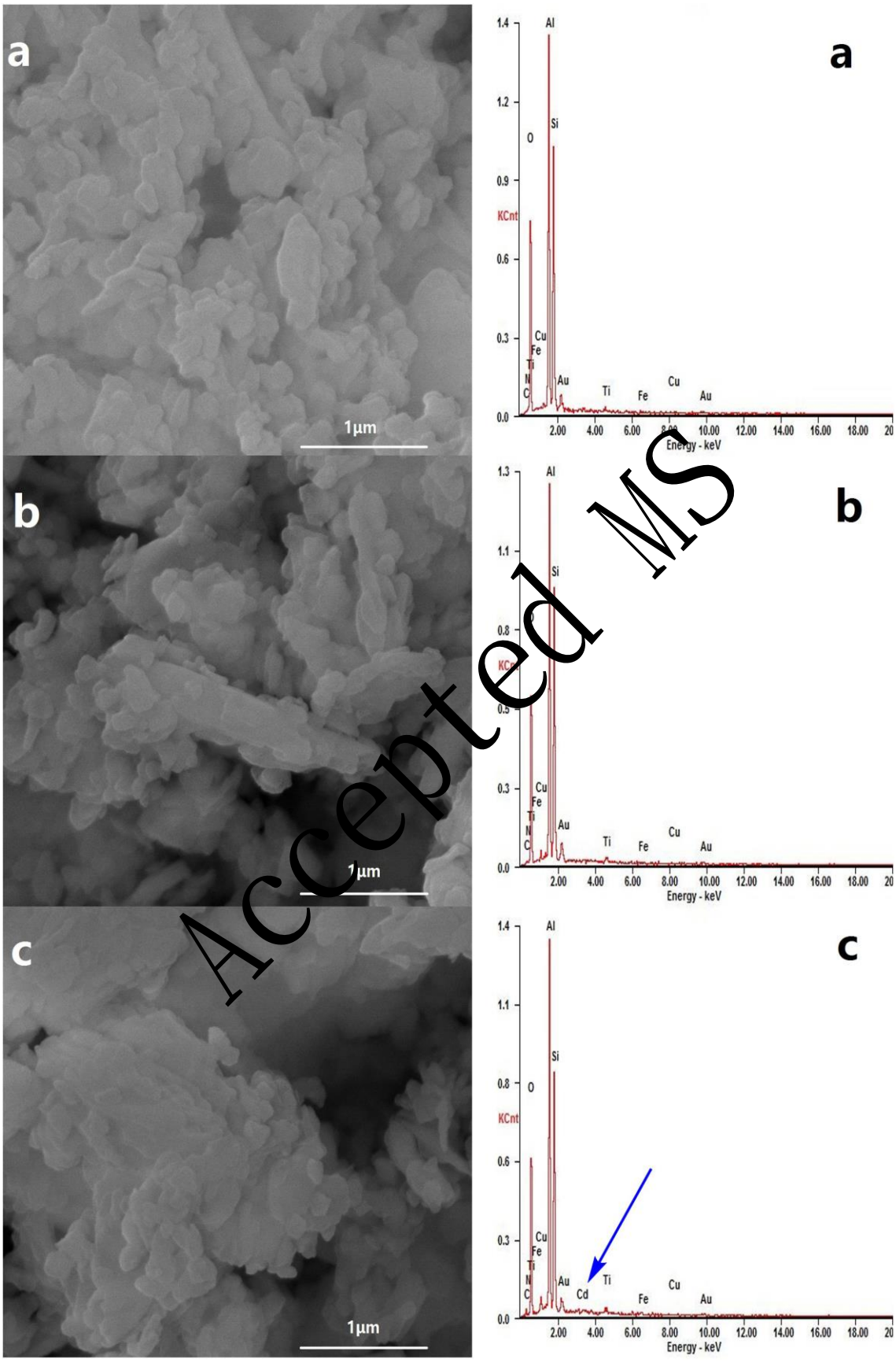

170

Fig. 2. SEM images and relevant EDS of the a) kaolinite, b) Kaolin-*Lac*, c) Kaolin-*Lac* after treatment.

Table 1.The element analysis of kaolinite, Kaolin-Lac, Kaolin-*Lac* after treatment

Element / Samples	C %	O %	Al %	Si %	Fe %	Cu %	Ti %	Cd %
Kaolinite	1.89	40.76	27.28	27.77	0.71	0.62	0.97	0
Kaolin-*Lac*	2.84	37.72	27.87	29.08	0.63	0.66	1.18	0
Kaolin-*Lac* after treatment	3.18	40.13	26.64	27.45	0.73	0.66	0.97	0.21

3.1.2. FTIR analysis.

The FTIR spectra of kaolinite, Kaolin-*Lac* and Kaolin-*Lac* after treatment were shown in Fig. 3. Infrared spectrum determines the quantity of radiation absorbed by atoms at different frequencies (Chen et al., 2017; Huang et al., 2017b). Whilst the infrared radiation irradiated the compound, the dissimilarity of charge between carbon atoms evokes the formation of an electric dipole that can form detectable signals (Cheng et al., 2016; Huang et al., 2016). FT-IR spectras of the powder samples (Fig. 3) were surveyed with KBr pellets in the scope of 500-4000 cm^{-1}.

Some clear adsorption bands among all samples confirmed that Si-OH and Al-OH were existed in these samples. Among the sample of Kaolinite and Kaolin-Lac, a clear band peak in 3779 cm^{-1} can be ascribed to the vibration of Si-OH (Shu et al., 2016; Ztrk et al., 2008). Another adsorption band at 1627 cm^{-1} belongs to the stretching vibration of H-OH, which was crystal water molecules in the lattice (Wen et al., 2018; Chen et al., 2017; Xue et al., 2018). Absorption bands around 1170 cm^{-1}, 827 cm^{-1}, 570 cm^{-1} of spectrum a, b, c are assigned to the bending vibration of Si-O, respectively (Huang et al., 2018b; Shu et al., 2016). The adsorption bands among the range of 400-500 cm^{-1} were belonging to the group of Si-O and Al-O (Shu et al., 2016). After immobilization and treatment, a red shift occurred on the group of Si-O, Si-OH and H-OH. This phenomenon indicated that the surface groups became unstable after immobilization and treatment (Andjelkovi et al., 2015). Due to the "broken-bond" surface, kaolinite has certain of cation exchange capacity. There are a large number of negative charges on $Si\text{-}O^-$ and $Al\text{-}O^-$ groups (Tan et al., 2018). The loading of laccase on kaolinite, the adsorption of Cd (II) on kaolinite and the adsorption or degradation of MG on kaolinite could occupy the binding sites of the exchangeable cations and thus lead to the change on surface charge density of Kaolinite (Huang et al., 2018c). At the same time, the π

199 interactions between the oxygen plane of the aluminosilicate layer of the clay mineral
200 and MG, decrease of inner surface hydroxyl group due to the prototropy also could lead
201 to the instability of different surface groups (Johnston et al., 1984). As a whole, it means
202 that immobilization of laccase on kaolinite and degradation of MG effluent coexisting
203 with Cd (II) on the surface of kaolinite had a certain influence on surface functional
204 groups of kaolinite.

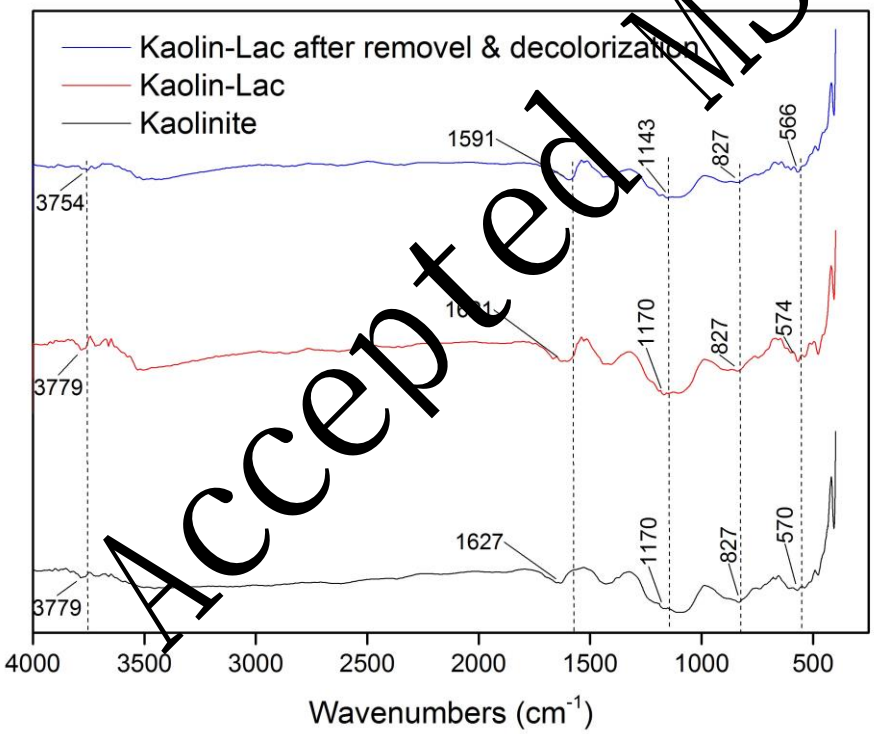

205

206 **Fig. 3.** FT-IR spectrum of kaolinite, Kaolin-*Lac*, Kaolin-*Lac* after treatment.

207 **3.2. Optimum Conditions of Laccase Immobilization.**

208 Laccase immobilization process is affected by many factors (Liu et al., 2012). The
209 initial laccase concentration had great influence on the immobilization process. To study

the influence of the initial laccase concentration on the activity of immobilized laccase, the initial laccase concentration was varied from 0.01 mg/mL to 1 mg/mL. As shown in Fig.4a, the adsorbed laccase increased with the increase of initial laccase concentration. However, the activity of immobilized laccase increased until 0.8 mg/mL, whilst the laccase concentration was larger than 0.8 mg/mL, a decrease in the relative activity of the Kaolin-*Lac* was observed. Similar phenomenon was also observed for some previous supporting materials (Kadam et al., 2017; Liu et al., 2012). This could ascribe to the agglomeration or crowding of enzyme molecules onto the surface of kaolinite when the laccase was overloaded on the kaolinite (Cong et al., 2017; Liu et al., 2012). The agglomeration or crowding of laccase molecules on surface of kaolinite could constraint the dispersion and transmission of laccase, even change the conformation of laccse and thus lead to the change of laccse activity. Thus, the appropriate laccase concentration was set as 0.8 mg/mL for next studies.

The immobilization time also remarkably influences the immobilization laccase activity (Huang et al., 2017c; Zheng et al., 2016). As demonstrated in Fig.4b, the relative activity of Kaolin-*Lac* changed with the immobilization time increased from 15 min to 300 min. The relative activity of Kaolin-*Lac* increased strikingly until 180min,

and then the relative activity decreased (Huang et al., 2018d). Activity of immobilized enzymes seemed to rely on the nature of the protein. With time increasing, the possible inactivation amounts of laccase increased during immobilization. In the meantime, the laccase flexibility also reduced. As physical adsorption immobilization time increased, the adsorption site on kaolinite was eliminated (Huang et al., 2017d). The relevant steric hindrance and diffusion limitations might also lead to loss of laccase activity (Prasad and Palanivelu, 2015). The optimum immobilization time was 180 min. Under above optimal condition, the acquired immobilized laccase (Kaolin-*Lac*) could achieve a loading efficiency of 88.22%, a loading capacity of 12.55 mg/g, and the highest enzyme activity of 839.01 U/g.

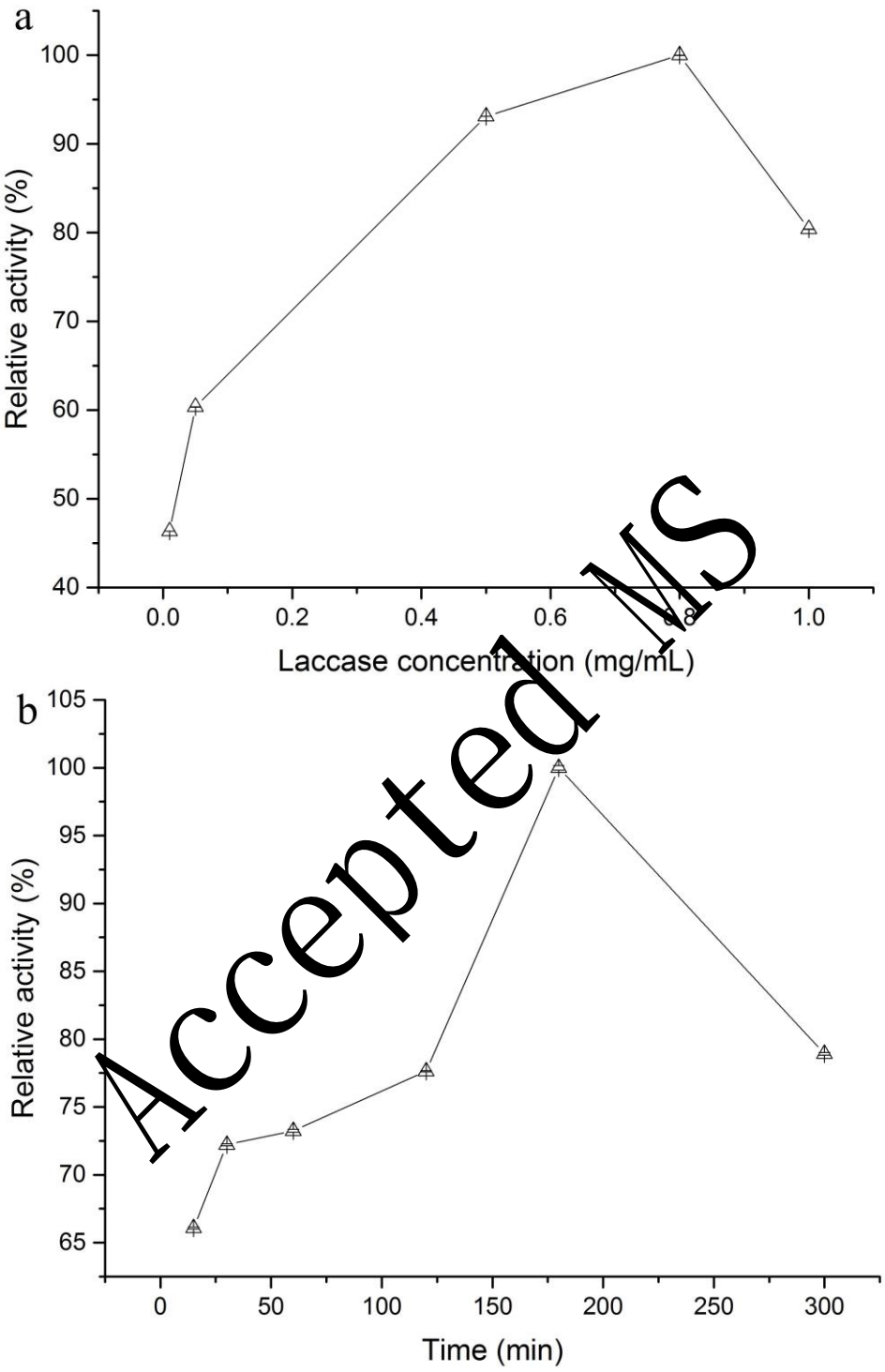

237

238 **Fig.4**. a) Effect of laccase concentration on the activity of the immobilized laccase; b)

239 Effect of time on the activity of the immobilized laccase.

3.3. Properties of Immobilized Laccase.

3.3.1. pH stability.

The pH stability of immobilized laccase is a key factor for practical use (Mahmoodi et al., 2014). The results presented in Fig.5a showed that the Kaolin-*Lac* exhibited more stable relative activity over a broad pH range from 3.0 to 6.0. The minimum relative activity of Kaolin-*Lac* could maintain more than 60%. And the relative activity of free laccase was strikingly decreased from pH 3.0. When pH value was 6, the relative activity of free laccase almost decreased to 2%. The phenomenon suggested that immobilization of laccase improved its pH stability and enhanced its adaptive capacity to the environment. The change of pH stability could be ascribed to the proton production on the surface of support. Relative stable proton production could retain the activity of laccase. The laminated structure of kaolinite maintained a balance proton quantity in the microenvironment around the laccase. This causation could explain the higher pH stability of Kaolin-*Lac* (Skoronski et al., 2017).

3.3.2. Thermal stability.

The thermal stability of immobilized laccase is important for its practical application as biocatalyst (Li et al., 2016). As showed in Fig.5b, when the temperature

was lower than 40 ℃, the activity of Kaolin-*Lac* was increasing with the increase of temperature. Kaolin-*Lac* showed its highest stability at 40 ℃. Then the activity of Kaolin-*Lac* began to decrease. From 20 ℃ to 80 ℃, the relative activity of free laccase was decreased all the way. Especially, the activity of free laccase strikingly decreased when temperature was higher than 50 ℃. And free laccase nearly lost its activity when the temperature was higher than 70 ℃. However, when temperature was higher than 50 ℃, the Kaolin-*Lac* decreased more tardily and Kaolin-*Lac* could still maintain 18% of its original activity when temperature was 80 ℃. Obviously, immobilization process improved the tolerance of laccase for high temperature. The phenomenon was attributed to the augment of enzyme rigidity and decrease of conformational enzyme flexibility which was caused by the high stability towards denaturation on enzyme by high temperatures. Similarly, the results can be ascribed to the stronger physical bond between the supports and enzyme or the lower restriction of substrate diffusion when the temperature was high (Andjelkovi et al., 2015). The improved thermal stability of immobilized laccase is beneficial to its practical application because the industrial waste water was usually high temperatures (Chang et al., 2016).

3.3.3. Storage stability

Storage stability is of key influence on the practical utilize of immobilized enzyme (Wang et al., 2013). Generally, the free enzyme is not stable and it could lose its activity by degrees during storage period (Chang et al., 2016). The free and immobilized laccase were kept at 4 for 30 days and their activities were measured per five days to analyze their storage stability. The results were depicted in Fig. 5c and confirmed that the Kaolin-*Lac* had higher storage stability than the free laccase. During the whole 30 days, nearly 40% activity was retained for Kaolin-Lac whilst almost only 20% activity of free laccase was retained. Similar increases of storage stability have been reported by Asgher et al. and Ghiaci et al. after immobilizing laccase on chitosan microspheres and bentonite (Asgher et al., 2017; Ghiaci et al., 2009). The improvement in storage stability of immobilized laccase can be ascribed to the structural rigidness of laccase, the stabilization of support and the protection of laccase from unfolding and denaturation by supports (Andjelkovi et al., 2015).

3.3.4. Operational stability and reusability

The operational stability and reusability of immobilized laccase are of important significances for practical use. The operational stability and reusability of Kaolin-*Lac*

was explored through a series of cyclic experiments using ABTS as standard substrate and degraded MG effluent with the coexistence of Cd (II). The results shown in Fig. 5d, the Kaolin-*Lac* lost nearly 50% of its activity after 2 cycles and then the Kaolin-*Lac* could maintain nearly 50% of its initial activity. The Kaolin-*Lac* could retain nearly 80% decolorization for MG after five cycles. The physical adsorption immobilization had weak bonds between enzyme and support, hence, the loss of enzyme activity can be ascribed to the enzyme leaching during washing process (Liu et al., 2012). However, the laccase sited in the slit of kaolinite was difficult to leak, which resulted in a relatively stable operational stability (Zheng et al., 2016). The stable operational stability could afford stable degradation ability for MG. Immobilization could provide protection for laccase through the carrier kaolinite and retained laccase activity and the degradation ability for MG.

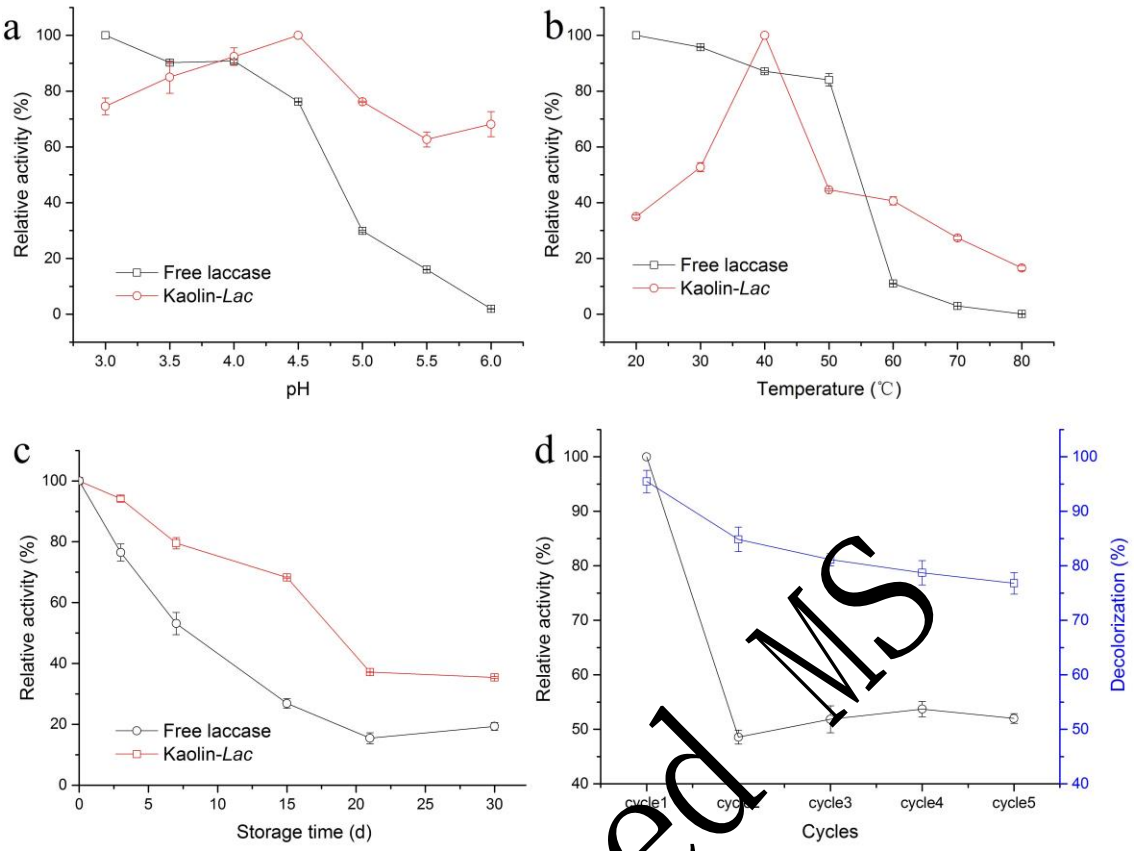

Fig. 5. a) pH stability of free laccase and Kaolin-*Lac*; b) Thermal stability studies of free laccase and Kaolin-*Lac* at 20-80 ℃ up to 120 min; c) Storage stability of free laccase and Kaolin-*Lac*; d) Operational stability of Kaolin-*Lac* and reusability of Kaolin-*Lac* for MG with the coexistence of Cd (II) decolorization.

3.4. Treatment of MG Effluent mixing with Cd (II).

3.4.1. Effect of concentration of SA

The existence of mediator SA could markedly improve the react velocity. The mediator could decrease the energy required for the reaction need, thus accelerating reaction (Murugesan et al., 2009). The Fig. 6a and Fig. 6b demonstrated the effect of

312 different concentrations of mediator SA on the decolorization of MG mixed with Cd (Π).
313 As shown in the Fig.6a, the decolorization of MG had been strikingly improved while
314 the concentration of SA changed from 0 to 0.5 mg/L. However, the decolorization of
315 MG by Kaolin-*Lac* began to decrease when the concentration of SA exceeded 0.5 mg/L.
316 This phenomenon demonstrated that the concentration of SA was important for
317 decolorization of MG by Kaolin-*Lac*. And the optimum concentration of SA could
318 provide moderate amount for the oxidation reduction cycle of laccase which was
319 immobilized on the kaolinite (Chhabra et al., 2009). Superfluous mediator, SA, which
320 couldn't be oxidized by laccase might possess toxicity to laccase. In the Fig. 6b, the
321 concentration of SA had little influence on the removal of Cd (Π). This result can be
322 ascribed to which the removal of Cd (Π) was the adsorption function of kaolinite and
323 laccase. The adsorption ability had nothing with the activity of laccase, hence, the
324 concentration of SA had little effect on the removal of Cd (II).
325 3.4.2. Effect of concentration of Cd (Π)
326 Generally, metal ions could bind with the enzyme and change the activity of
327 enzyme (Jadhav et al., 2010). Different types and concentrations of metal ions have
328 different influence on the laccase activity. Most of them had negative effect on laccase.

But several studies confirmed that free laccase had tolerance to different concentration of Ca (Π), Mg (Π), Cu (Π) and Mn (Π) (Casas et al., 2009; Wang et al., 2017). As a common deleterious metal, Cd (Π) is often mixed in the textile industries. Some studies have reported that free laccase has tolerance to Cd (Π) (Casas et al., 2009; Jadhav et al., 2010). However, there were few reports about the influence of Cd (Π) on the degradation of MG effluent by immobilized laccase. The property of laccase may change after immobilization. The effects of Cd (II) on activity of laccase maybe also change. As depicted in the Fig. 6c, when the concentration of Cd (Π) was lower than 5 mg/L, the decolorization of Kaolin-Lac for MG increased as concentration of Cd (Π) increased. When the concentration of Cd (Π) ranged from 5 mg/L to 20 mg/L, the decolorization of Kaolin-Lac for MG was unstable. When the concentration of Cd (Π) was higher than 20 mg/L, the decolorization of Kaolin-Lac for MG maintained with nearly 75%. This phenomenon demonstrated that low contration of Cd (II) could improve the decolorization of Kaolin-*Lac* for MG, and high concentration of Cd (II) didn't strikingly decrease the decolorization of Kaolin-Lac for MG. It indicated that Kaolin-*Lac* also had certain tolerance to Cd (Π) and the immobilization process had little effect on the tolerance of laccase for Cd (Π). From the Fig. 6d, it could be seen that

346 Kaolin-*Lac* had certain removal ability for Cd (Π). Comparing with kaolinite, the
347 Kaolin-*Lac* had higher removal ability for Cd (Π). When the concentration of Cd (Π)
348 was 40 mg/L, Kaolin-*Lac* had the highest removal efficiency of Cd (Π), which was
349 close to 23%. The higher removal ability for Cd (Π) of Kaolin-*Lac* could be attributed
350 to the synergetic effect of kaolinite and laccase (Yang et al., 2017). Immobilization of
351 laccase on kaolinite might change the surface charge density, surface functional groups
352 of kaolinite that confirmed by FTIR results, leading to the change of adsorption ability
353 of kaolinite. Also, laccase could interact with Cd (II) through the Vander waals
354 adsorption or hydrogen bond adsorption.

355 3.4.3. Effect of time

356 The Fig. 6e and Fig. 6f districted the decolorization of MG mixing with Cd (Π) in
357 a 5 h successive experiment. By contrast, the decolorization of MG and the removal of
358 Cd (Π) by kaolinite were compared. As shown in Fig. 6e, the decolorization of MG by
359 Kaolin-*Lac* could achieve 74% after 15 min incubation. As the decolorization time
360 increased, the decolorization velocity became slow. After 300 min incubation, MG was
361 nearly decolorized totally. However, the kaolinite only achieved 10% decolorization
362 after 5 h reaction. This phenomenon could confirm the more important contribution of

363 the laccase catalytic process for decolorization of MG. And with time increasing, the
364 lower decolorization velocity might attribute to the effect of the accumulation of
365 degradation products on laccase activity. As depicted in Fig. 6f, the removal of Cd (Π)
366 by Kaolin-*Lac* and kaolinite demonstrated 21% and 19%, separately. The higher
367 removal ability of Kaolin-*Lac* might be ascribed to the adsorption of ions by laccase and
368 the change of adsorption ability of kaolinite (Chen et al., 2017; Zeng et al., 2017). As
369 shown in Fig. 6, the removal of MG and Cd (Π) could be attributed to the united effects
370 of degradation by the laccase and the adsorption by the kaolinite support (Yang et al.,
371 2017).

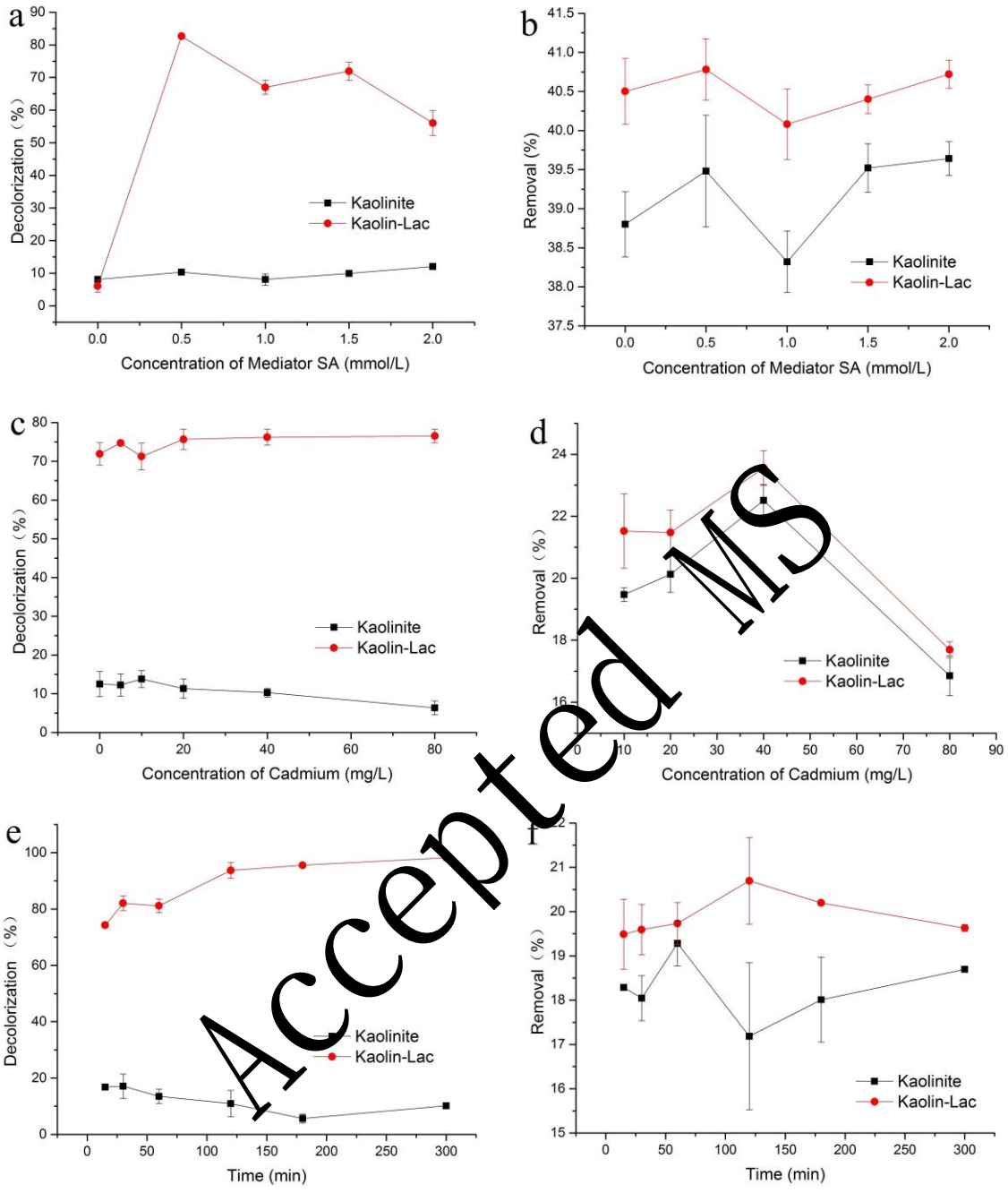

372

373 **Fig. 6.** a)&b) Effect of concentration of mediator SA on treatment of MG effluent

374 mixing with Cd (Π) by Kaolin-*Lac*; c)&d)Effect of concentration of cadmium on

375 treatment of MG effluent mixing with Cd (Π) by Kaolin-*Lac*; e)&f)Effect of time on

376 removal rates of MG effluent mixing with Cd (Π) by Kaolin-*Lac*.

4. Conclusion

This study demonstrated the gradual progress of immobilizing laccase on kaolinite. Successful preparation of Kaolin-*Lac* was confirmed by structural characterizations using FT-IR, SEM-EDS. The stabilities of Kaolin-*Lac* were enhanced compared to free laccase. The Kaolin-*Lac* retained 50% of the original activity and nearly 80% decolorization for MG after 5 cycles. In the presence of mediator SA, the Kaolin-*Lac* used to degrade MG exhibited nearly 100% in 300 minutes, and almost 25% removal for Cd (Π). This study confirms that kaolinite can serve as microreactor for biomacromolecule immobilization. The low concentration coexistence of Cd (II) could improve the degradation of MG by Kaolin-*Lac*. Kaolin-*Lac* had certain tolerance to high concentration of Cd (II). As obtained Kaolin-*Lac* is an economically, ecofriendly biocatalyst, it has extensive applicability for the treatment of MG effluent mixing with Cd (Π).

Acknowledgements

This study was financially supported by the Program for the National Natural Science Foundation of China (51521006, 51579098, 5110916, 51378190, 51278176,

51408206), The Natural Science Foundation of Hunan province (2018JJ3549), the National Program for Support of Top-Notch Young Professionals of China (2014), the Fundamental Research Funds for the Central Universities, the Hunan Provincial Science and Technology Plan Project (2017SK2361, 2016RS3026), the Hunan Province Water Conservancy Science and Technology Project ([2016] 194-12, [2017] 230-22), the Program for New Century Excellent Talents in University (NCET-13-0186), the Program for Changjiang Scholars and Innovative Research Team in University (IRT-13R17), the Scientific Research Fund of Hunan Provincial Education Department (No.521293050).

References

Abdul Rahman, M.B., Tajuddin, S.M., Hussein, M.Z., Abdul Rahman, R.N.Z.R., Salleh, A.B., Basri, M., 2005. Application of natural kaolin as support for the immobilization of lipase from Candida rugosa as biocatalsyt for effective esterification. Appl. Clay Sci. 29, 111-116.

An, N., Zhou, C.H., Zhuang, X.Y., Tong, D.S., Yu, W.H., 2015. Immobilization of enzymes on clay minerals for biocatalysts and biosensors. Appl. Clay Sci. 114, 283-296.

413 Andjelkovi, U., Milutinovi Nikoli, A., Jovi Jovi I, N.A., Bankovi, P., Bajt, T., Mojovi,
414 Z., Vuj I, Z., Jovanovi, D.A., 2015. Efficient stabilization of Saccharomyces
415 cerevisiae external invertase by immobilisation on modified beidellite nanoclays.
416 Food Chem. 168, 262-269.
417 Asgher, M., Noreen, S., Bilal, M., 2017. Enhancing catalytic functionality of Trametes
418 versicolor IBL-04 laccase by immobilization on chitosan microspheres. Chem. Eng.
419 Res. Des. 119, 1-11.
420 Barbosa, O., Torres, R., Ortiz, C., Berenguer-Murcia, N., Rodrigues, R.C.,
421 Fernandez-Lafuente, R., 2013. Heterofunctional Supports in Enzyme Immobilization:
422 From Traditional Immobilization Protocols to Opportunities in Tuning Enzyme
423 Properties. Biomacromolecules. 14, 2433-2462.
424 Casas, N., Parella, T., Vicent, T., Caminal, G., Sarra, M., 2009. Metabolites from the
425 biodegradation of triphenylmethane dyes by Trametes versicolor or laccase.
426 Chemosphere. 75, 1344-1349.
427 Chang, Y., Lee, J., Liu, K., Liao, Y., Yang, V., 2016. Immobilization of fungal laccase
428 onto a nonionic surfactant-modified clay material: application to PAH degradation.
429 Environ. Sci. Pollut. R. 23, 4024-4035.

Chen, J., Leng, J., Yang, X., Liao, L., Liu, L., Xiao, A., 2017. Enhanced Performance of Magnetic Graphene Oxide-Immobilized Laccase and Its Application for the Decolorization of Dyes. Molecules. 22, 221

Chen, M., Xu, P., Zeng, G., Yang, C., Huang, D., Zhang, J., 2015. Bioremediation of soils contaminated with polycyclic aromatic hydrocarbons, petroleum, pesticides, chlorophenols and heavy metals by composting: Applications, microbes and future research needs. Biotechnol. Adv. 33, 745-755.

Chen, Y., Peng, J., Xiao, H., Peng, H., Bu, L., Pan, Z., He, Y., Chen, F., Wang, X., Li, S., 2017. Adsorption behavior of hydrotalcite-like modified bentonite for Pb^{2+}, Cu^{2+} and methyl orange removal from water. Appl. Surf. Sci. 420, 773-781.

Cheng, M., Zeng, G., Huang, D., Lai, C., Xu, P., Zhang, C., Liu, Y., 2016. Hydroxyl radicals based advanced oxidation processes (AOPs) for remediation of soils contaminated with organic compounds: A review. Chem. Eng. J. 284, 582-98.

Cheng, Y., He, H., Yang, C., Zeng, G., Li, X., Chen, H., Yu, G., 2016. Challenges and solutions for biofiltration of hydrophobic volatile organic compounds. Biotechnol. Adv. 34, 1091-1102.

Chhabra, M., Mishra, S., Sreekrishnan, T.R., 2009. Laccase/mediator assisted

447 degradation of triarylmethane dyes in a continuous membrane reactor. J. Biotechnol.
448 143, 69-78.
449 Datta, S., Christena, L.R., Rajaram, Y.R.S., 2013. Enzyme immobilization: an overview
450 on techniques and support materials. 3 Biotech. 3, 1-9.
451 Deng, J., Zhang, X., Zeng, G., Gong, J., Niu, Q., Liang, J., 2013. Simultaneous removal
452 of Cd(II) and ionic dyes from aqueous solution using magnetic graphene oxide
453 nanocomposite as an adsorbent. Chem. Eng. J. 226, 189-200.
454 Ghiaci, M., Aghaei, H., Soleimanian, S., Sedaghat, M.E., 2009. Enzyme immobilization:
455 Part 2. Immobilization of alkaline phosphatase on Na-bentonite and modified
456 bentonite. Appl. Clay Sci. 43, 308-316.
457 Gong, J.L., Wang, B., Zeng, G.M., Yang, C.P., Niu, C.G., Niu, Q.Y., Zhou, W.J., Liang,
458 Y., 2009. Removal of cationic dyes from aqueous solution using magnetic multi-wall
459 carbon nanotube nanocomposite as adsorbent. J. Hazard. Mater. 164, 1517-22.
460 Gong, X., Huang, D., Liu, Y., Zeng, G., Wang, R., Wan, J., Zhang, C., Cheng, M., Qin,
461 X., Xue, W., 2017. Stabilized Nanoscale Zerovalent Iron Mediated Cadmium
462 Accumulation and Oxidative Damage of *Boehmeria nivea (L.) Gaudich* Cultivated in
463 Cadmium Contaminated Sediments. Environ. Sci. Technol. 51, 11308-11316.

464 Guzik, U., Hupert-Kocurek, K., Wojcieszyska, D., 2014. Immobilization as a Strategy
465 for Improving Enzyme Properties-Application to Oxidoreductases. Molecules. 19,
466 8995-9018.
467 Hu, X., Zhao, X., Min Hwang, H., 2007. Comparative study of immobilized Trametes
468 versicolor laccase on nanoparticles and kaolinite. Chemosphere. 66, 1618-1626.
469 Huang, D., Deng, R., Wan, J., Zeng, G., Xue, W., Wen, X., Zhou, C., Hu, L., Liu, X.,
470 Xu, P., Guo, X., Ren, X., 2018. Remediation of lead-contaminated sediment by
471 biochar-supported nano-chlorapatite: Accompanied with the change of available
472 phosphorus and organic matters. J. Hazard. Mater. 348, 109-116.
473 Huang, D., Gong, X., Liu, Y., Zeng, G., Lai, C., Bashir, H., Zhou, L., Wang, D., Xu, P.,
474 Cheng, M., Wan, J., 2017. Effects of calcium at toxic concentrations of cadmium in
475 plants. Planta. 245, 863-873.
476 Huang, D., Guo, X., Peng, Z., Zeng, G., Xu, P., Gong, X., Deng, R., Xue, W., Wang, R.,
477 Yi, H., Liu, C., 2018. White rot fungi and advanced combined biotechnology with
478 nanomaterials:promising tools for endocrine-disrupting compounds biotransformation.
479 Crit. Rev. Biotechnol. 38, 671-689.
480 Huang, D., Hu, C., Zeng, G., Cheng, M., Xu, P., Gong, X., Wang, R., Xue, W., 2017.

Combination of Fenton processes and biotreatment for wastewater treatment and soil remediation. Sci. Total Environ. 574, 1599-1610.

Huang, D., Hu, Z., Peng, Z., Zeng, G., Chen, G., Zhang, C., Cheng, M., Wan, J., Wang, X., Qin, X., 2018. Cadmium immobilization in river sediment using stabilized nanoscale zero-valent iron with enhanced transport by polysaccharide coating. J. Environ. Manage. 210, 191-200.

Huang, D., Liu, L., Zeng, G., Xu, P., Huang, C., Deng, L., Wang, R., Wan, J., 2017. The effects of rice straw biochar on indigenous microbial community and enzymes activity in heavy metal-contaminated sediment. Chemosphere. 174, 545-553.

Huang, D., Wang, R., Wang, X., Zhang, C., Zeng, G., Peng, Z., Zhou, J., Cheng, M., Hu, Z., Qin, X., 2017. Sorptive removal of ionizable antibiotic sulfamethazine from aqueous solution by graphene oxide-coated biochar nanocomposites: Influencing factors and mechanism. Chemosphere. 186, 414-421.

Huang, D., Xue, W., Zeng, G., Wan, J., Chen, G., Huang, C., Zhang, C., Cheng, M., Xu, P., 2016. Immobilization of Cd in river sediments by sodium alginate modified nanoscale zero-valent iron: Impact on enzyme activities and microbial community diversity. Water Res. 106, 15-25.

498 Huang, D., Yan, X., Yan, M., Zeng, G., Zhou, C., Wan, J., Cheng, M., Xue, W., 2018.
499 Graphitic Carbon Nitride-Based Heterojunction Photoactive Nanocomposites:
500 Applications and Mechanism Insight. ACS Appl. Mater. Inter. 10, 21035-21055.
501 Jadhav, J.P., Kallyani, D.C., Telke, A.A., Phugare, S.S., Govindwar, S.P., 2010.
502 Evaluation of the efficacy of a bacterial consortium for the removal of color,
503 reduction of heavy metals, and toxicity from textile dye effluent. Bioresource
504 Technol. 101, 165-173.
505 Jasinska, A., Rozalska, S., Bernat, P., Paraszkiewicz, K., Dlugonski, J., 2012. Malachite
506 green decolorization by non-basidiomycete filamentous fungi of Penicillium
507 pinophilum and Myrothecium roridum. Int. Biodeter. Biodegr. 73, 33-40.
508 Johnston, C.T., Sposito, G., Bocian, D.F., Birge, R.R., 1984. Vibrational spectroscopic
509 study of the interlamellar kaolinite-dimethyl sulfoxide complex. The Journal of
510 Physical Chemistry. 88, 5959-5964.
511 Kadam, A.A., Jang, J., Lee, D.S., 2017. Supermagnetically Tuned Halloysite Nanotubes
512 Functionalized with Aminosilane for Covalent Laccase Immobilization. ACS Appl.
513 Mater. Inter. 9, 15492-15501.
514 Kuhar, F., Castiglia, V., Levin, L., 2015. Enhancement of laccase production and

malachite green decolorization by co-culturing Ganoderma lucidum and Trametes versicolor in solid-state fermentation. Int. Biodeter. Biodegr. 104, 238-243.

Kumar, V.V., Sivanesan, S., Cabana, H., 2014. Magnetic cross-linked laccase aggregates - Bioremediation tool for decolorization of distinct classes of recalcitrant dyes. Sci. Total Environ. 487, 830-839.

Li, G.H., Nandgaonkar, A.G., Lu, K.Y., Krause, W.E., Lucia, L.A., Wei, Q.F., 2016. Laccase immobilized on PAN/O-MMT composite nanofibers support for substrate bioremediation: a de novo adsorption and biocatalytic synergy. RSC Adv. 6, 41420-41427.

Liang, J., Yang, Z., Tang, L., Zeng, G., Yu, M., Li, X., Wu, H., Qian, Y., Li, X., Luo, Y., 2017. Changes in heavy metal mobility and availability from contaminated wetland soil remediated with combined biochar-compost. Chemosphere. 181, 281-288.

Liu, Y.Y., Zeng, Z.T., Zeng, G.M., Tang, L., Pang, Y., Li, Z., Liu, C., Lei, X.X., Wu, M.S., Ren, P.Y., Liu, Z.F., Chen, M., Xie, G.X., 2012. Immobilization of laccase on magnetic bimodal mesoporous carbon and the application in the removal of phenolic compounds. Bioresource Technol. 115, 21-26.

Long, F., Gong, J., Zeng, G., Chen, L., Wang, X., Deng, J., Niu, Q., Zhang, H., Zhang, X., 2011. Removal of phosphate from aqueous solution by magnetic Fe-Zr binary oxide. Chem. Eng. J. 171, 448-455.

Mahmoodi, N.M., Arabloo, M., Abdi, J., 2014. Laccase immobilized manganese ferrite nanoparticle: Synthesis and LSSVM intelligent modeling of decolorization. Water Res. 67, 216-226.

Mohamad, N.R., Marzuki, N.H.C., Buang, N.A., Huyop, F., Wahab, R.A., 2015. An overview of technologies for immobilization of enzymes and surface analysis techniques for immobilized enzymes. Biotechnol. Biotec. Eq. 29, 205-220.

Murugesan, K., Yang, I., Kim, Y., Jeon, J., Chang, Y., 2009. Enhanced transformation of malachite green by laccase of Ganoderma lucidum in the presence of natural phenolic compounds. Appl. Microbiol. Biot. 82, 341-350.

Prasad, M., Palanivelu, P., 2015. Immobilization of a thermostable, fungal recombinant chitinase on biocompatible chitosan beads and the properties of the immobilized enzyme. Biotechnol. Appl. Bioc. 62, 523-529.

Ren, X., Zeng, G., Tang, L., Wang, J., Wan, J., Liu, Y., Yu, J., Yi, H., Ye, S., Deng, R., 2018. Sorption, transport and biodegradation-An insight into bioavailability of

549 persistent organic pollutants in soil. Sci. Total Environ. 610-611, 1154-1163.

550 Sheldon, R.A., van Pelt, S., 2013. Enzyme immobilisation in biocatalysis: why, what

551 and how. Chem. Soc. Rev. 42, 6223-6235.

552 Shu, Z., Li, T., Zhou, J., Chen, Y., Sheng, Z., Wang, Y., Yuan, X., 2016. Mesoporous

553 silica derived from kaolin: Specific surface area enlargement via a new

554 zeolite-involved template-free strategy. Appl. Clay Sci. 123, 76-82.

555 Shu, Z., Li, T., Zhou, J., Chen, Y., Yu, D., Wang, Y., 2014. Template-free preparation

556 of mesoporous silica and alumina from natural kaolinite and their application in

557 methylene blue adsorption. Appl. Clay Sci. 102, 33-40.

558 Sinegani, A.S., Emtiazi, G., Shariatmadari, H., 2005. Sorption and immobilization of

559 cellulase on silicate clay minerals. J. Colloid Interf. Sci. 290, 39-44.

560 Sinha, A., Osborne, W.J., 2016. Biodegradation of reactive green dye (RGD) by

561 indigenous fungal strain VITAF-1. Int. Biodeter. Biodegr. 114, 176-183.

562 Skoronski, E., Souza, D.H., Ely, C., Broilo, F., Fernandes, M., Junior, A.F., Ghislandi,

563 M.G., 2017. Immobilization of laccase from Aspergillus oryzae on graphene

564 nanosheets. Int. J. Biol. Macromol. 99, 121-127.

565 Sun, H.F., Yang, H., Huang, W.G., Zhang, S.J., 2015. Immobilization of laccase in a

566 sponge-like hydrogel for enhanced durability in enzymatic degradation of dye
567 pollutants. J. Colloid Interf. Sci. 450, 353-360.
568 Tan, D., Yuan, P., Dong, F., He, H., Sun, S., Liu, Z., 2018. Selective loading of
569 5-fluorouracil in the interlayer space of methoxy-modified kaolinite for controlled
570 release. Appl. Clay Sci. 159, 102-106.
571 Tan, X., Liu, Y., Zeng, G., Wang, X., Hu, X., Gu, Y., Yang, Z., 2015. Application of
572 biochar for the removal of pollutants from aqueous solutions. Chemosphere. 125,
573 70-85.
574 Tang, W., Zeng, G., Gong, J., Liang, J., Xu, P., Zhang, C., Huang, B., 2014. Impact of
575 humic/fulvic acid on the removal of heavy metals from aqueous solutions using
576 nanomaterials: A review. Sci. Total Environ. 468, 1014-1027.
577 Wan, J., Zeng, G., Huang, D., Hu, L., Xu, P., Huang, C., Deng, R., Xue, W., Lai, C.,
578 Zhou, C., Zheng, K., Ren, X., Gong, X., 2018. Rhamnolipid stabilized
579 nano-chlorapatite: Synthesis and enhancement effect on Pb-and Cd-immobilization in
580 polluted sediment. J. Hazard. Mater. 343, 332-339.
581 Wang, Q., Peng, L., Li, G., Zhang, P., Li, D., Huang, F., Wei, Q., 2013. Activity of
582 Laccase Immobilized on TiO_2-Montmorillonite Complexes. Int. J. Mol. Sci. 14,

12520-12532.

Wang, S., Ning, Y., Wang, S., Zhang, J., Zhang, G., Chen, Q., 2017. Purification, characterization, and cloning of an extracellular laccase with potent dye decolorizing ability from white rot fungus Cerrena unicolor GSM-01. Int. J. Biol. Macromol. 95, 920-927.

Wen, X., Du, C., Zeng, G., Huang, D., Zhang, J., Yin, L., Tan, S., Huang, L., Chen, H., Yu, G., Hu, X., Lai, C., Xu, P., Wan, J., 2018. A novel biosorbent prepared by immobilized Bacillus licheniformis for lead removal from wastewater. Chemosphere. 200, 173-179.

Wu, H., Lai, C., Zeng, G., Liang, J., Chen, J., Xu, J., Dai, J., Li, X., Liu, J., Chen, M., Lu, L., Hu, L., Wan, J., 2017. The interactions of composting and biochar and their implications for soil amendment and pollution remediation: a review. Crit. Rev. Biotechnol. 37, 754-764.

Xu, P., Zeng, G.M., Huang, D.L., Feng, C.L., Hu, S., Zhao, M.H., Lai, C., Wei, Z., Huang, C., Xie, G.X., Liu, Z.F., 2012. Use of iron oxide nanomaterials in wastewater treatment: A review. Sci. Total Environ. 424, 1-10.

Xu, P., Zeng, G.M., Huang, D.L., Lai, C., Zhao, M.H., Wei, Z., Li, N.J., Huang, C., Xie,

G.X., 2012. Adsorption of Pb(II) by iron oxide nanoparticles immobilized Phanerochaete chrysosporium: Equilibrium, kinetic, thermodynamic and mechanisms analysis. Chem. Eng. J. 203, 423-431.

Xue, W., Huang, D., Zeng, G., Wan, J., Zhang, C., Xu, R., Cheng, M., Deng, R., 2018. Nanoscale zero-valent iron coated with rhamnolipid as an effective stabilizer for immobilization of Cd and Pb in river sediments. J. Hazard. Mater. 341, 381-389.

Yang, J., Lin, Y.H., Yang, X.D., Ng, T.B., Ye, X.Y., Lin, J., 2017. Degradation of tetracycline by immobilized laccase and the proposed transformation pathway. J. Hazard. Mater. 322, 525-531.

Zeng, G., Wan, J., Huang, D., Hu, L., Huang, C., Cheng, M., Xue, W., Gong, X., Wang, R., Jiang, D., 2017. Precipitation, adsorption and rhizosphere effect: The mechanisms for Phosphate-induced Pb immobilization in soils-A review. J. Hazard. Mater. 339, 354-367.

Zhang, C., Lai, C., Zeng, G., Huang, D., Yang, C., Wang, Y., Zhou, Y., Cheng, M., 2016. Efficacy of carbonaceous nanocomposites for sorbing ionizable antibiotic sulfamethazine from aqueous solution. Water Res. 95, 103-112.

Zhang, Y., Zeng, G.M., Tang, L., Chen, J., Zhu, Y., He, X.X., He, Y., 2015.

617 Electrochemical Sensor Based on Electrodeposited Graphene-Au Modified Electrode
618 and NanoAu Carrier Amplified Signal Strategy for Attomolar Mercury Detection.
619 Anal. Chem. 87, 989-996.
620 Zheng, F., Cui, B.K., Wu, X.J., Meng, G., Liu, H.X., Si, J., 2016. Immobilization of
621 laccase onto chitosan beads to enhance its capability to degrade synthetic dyes. Int.
622 Biodeter. Biodegr. 110, 69-78.
623 Zhou, C., Lai, C., Huang, D., Zeng, G., Zhang, C., Cheng, M., Hu, L., Wan, J., Xiong,
624 W., Wen, M., Wen, X., Qin, L., 2018. Highly porous carbon nitride by
625 supramolecular preassembly of monomers for photocatalytic removal of
626 sulfamethazine under visible light driven. Applied Catalysis B: Environmental. 220,
627 202-210.
628 Ztrk, N., Tabak, A., Akgl, S., Denizli, A., 2008. Reversible immobilization of catalase
629 by using a novel bentonite-cysteine (Bent-Cys) microcomposite affinity sorbents.
630 Colloids and Surfaces A: Physicochemical and Engineering Aspects. 322, 148-154.
631